THE ASTROPHYSICAL JOURNAL 241:946–964, 1980 November 1

N-BODY SIMULATIONS OF SLOW TIDAL ENCOUNTERS AND THE FORMATION OF GALACTIC HALOS

AVISHAI DEKEL,[1] MYRON LECAR,[2] AND JACOB SHAHAM[1]

Received 1980 March 24; accepted 1980 April 29

ABSTRACT

Slow hyperbolic encounters, between a 250-body spherical system (a "halo") and a few-body perturber of comparable total mass, are studied by means of N-body simulations. The tidal effect on a system which initially has a decreasing $M(R)/R$ profile ($\rho \propto R^{-3}$) is to produce, or extend, an inner region of constant M/R, to encompass 50–70% of the bound mass. In the process, gradual stripping of up to one-third of the stars from the regions outside the half-radius R_h takes place, and no relaxed extended envelope forms. The flat inner profile is retained under tandem encounters while the outer parts are continuously stripped. These tidal effects are important whenever the closest approach distance of the centers of mass is less than about $5R_h$, and whenever their relative velocities are not much larger than the internal dispersion velocities.

The relevance of this effect to the formation of galactic halos is discussed both in the context of the merger theory of smaller objects and in the context of interacting galactic-scale systems. It is suggested that the regions of flat rotation curves, which exist in halos around spiral galaxies, correspond to the inner parts of larger, dark, protohalos which have undergone such slow tidal encounters while in their hierarchical gravitational clustering process.

The rates of mass loss and energy exchange are investigated and compared with previous estimates. There is a net gain in the internal energy of the system in all cases studied, even though the mass loss is substantial. Results derived by impulsive approximation in the tidal limit are found to be valid even for such slow encounters, provided the closest approach distance stays above $2R_h$. It is shown that a system which consists of elongated stellar orbits is mostly affected by the first-order ("fluctuating") term of the tidal interaction, while the second order ("secular") term is dominant for a system which consists of less eccentric orbits.

Subject headings: galaxies: evolution — galaxies: formation — galaxies: structure — stars: stellar dynamics

I. INTRODUCTION

a) *The Galactic-Halo Problem*

The existence of dark massive halos around many spiral galaxies, both in the field and in small groups, is now widely accepted. For binary galaxies and for galaxies in small groups, halo existence is indicated from dynamical evidence (Ostriker, Peebles and Yahil, 1974; Turner 1976*a*, *b*; Gott and Turner 1976; Kirshner 1977; Yahil 1977; for a review see Faber and Gallagher 1979); but the more striking evidence comes from galactic rotation curves both in the optical band of stars (Rubin 1978; Rubin, Ford, and Thonnard 1980) and at the 21 cm line of neutral hydrogen (Roberts 1975*a*, *b*; Krumm and Salpeter 1977). Rotation curves are, in many cases, flat out to distances of order 50 kpc, far beyond the main visible body of the galaxy. A circular velocity which does not fall off with distance R from the galactic center indicates a dark halo whose mass, if spherically distributed, grows linearly with the radius and has thus a density profile which falls off as R^{-2}.

Although the nature of the dark material is not yet known, it seems not to be gaseous (cf. Bergeron and Gunn 1977; Rees 1978*a*, *b*; Peebles 1980) but rather composed of condensed bodies, which might be unevolved low-mass stars (so called Jupiters), dead remnants of old stars, primordial massive black holes, or something else, where the first possibility seems to gain some observational support in at least one case (Dekel and Shaham 1979). Therefore, an N-body code is probably a proper numerical tool for investigating these halos.

Several dynamical arguments, which show that these nongaseous halos cannot be too flattened (cf. Ostriker and Peebles 1973; Ostriker, Peebles, and Yahil 1974), make us favor the case of spherical $M \propto R$ halos. No matter what the nature of the compact objects in the halos, the extended profile of $M \propto R$ ($\rho \propto R^{-2}$) is somewhat of a puzzle since other visible spherical systems, such as elliptical galaxies and nuclear bulges of spiral galaxies, have a Hubble-like ($\rho \propto R^{-3}$) profile, which is also predicted by most theories for galaxy formation.

Galactic halos could have been formed in two alternative ways: either by accumulation of smaller systems (cf. White and Rees 1978; Dekel and Shaham 1980*b*) or directly by collapse of halo-size systems (for a review, see Gott 1977). Both pictures have difficulties in explaining

[1] Racah Institute of Physics, The Hebrew University of Jerusalen.
[2] Harvard-Smithsonian Center for Astrophysics, Cambridge, Massachusetts.

the halo profile: White (1978, 1979) has carried out N-body experiments which seemed to indicate that violent mergers of spherical systems, which occur when the systems overlap significantly, lead to Hubble-like profiles. Simple dissipationaless models for the collapse of a sphere of stars (Peebles 1970; Gott 1973; Aarseth and Lecar 1975) lead to even steeper profiles, and those flatten to Hubble-like profiles on taking into account star formation during the collapse (Larson 1974*a*, *b*, 1975) or cosmological infall of outer, loosely bound shells (Gott 1975). The time scale for two-body relaxation, which can lead to an R^{-2}, isothermal, density profile, is much longer than the Hubble time.

The only mechanism known so far which might lead to the formation of a $\rho \propto R^{-2}$ halo is the secondary cosmological infall, suggested by Gunn (1977) and Gott (1977). It has recently been shown by N-body simulations (Dekel, Kowitt, and Shaham 1980) that this mechanism might indeed produce such a profile, but it requires somewhat special initial conditions: (*a*) the central perturbation, which is the progenitor of the galaxy, needs to be initially embedded in a bound homogeneous background—an assumption which might not be fully justified for relatively isolated galaxies; and (*b*) the infall is required to be dissipationless, so that most of the mass must already be in form of compact objects prior to halo formation. Even though this mechanism may still operate in some cases, it seems necessary to look for an alternative mechanism which might be responsible for the $M \propto R$ profiles in small groups and in the field. This is likely to be either a single-galaxy mechanism, or it may be due to interaction with neighboring galaxies in rich clusters.

b) Tidal Encounters

By *slow hyperbolic* tidal interaction between stellar systems we describe a process in which the interaction time is not much shorter than the crossing times in each system. Such processes should be considered in the context of hierarchical gravitational clustering, whether encounters occur between preformed halos of galactic mass or between smaller objects (as a stage in their clustering to a halo). It is obvious that, in such an encounter, energy is exchanged between the two-body motion and the internal degrees of freedom of each system. This exchange causes partial disruption in each system and also effects their mass profile.

Slow encounters, in which the systems are initially bound or almost bound, lead to mergers. N-body simulations of the merging of two spherical systems have been carried out by White (1978, 1979), who was able to investigate density profiles, and by Roos and Norman (1979) using a smaller number of particles (~ 30).

Fast hyperbolic encounters, like those taking place in rich clusters of galaxies, were studied extensively by means of the impulsive approximation, in which the mass distribution within the unperturbed system was assumed not to change appreciably during the passage of the perturber. Spitzer (1958) has analytically estimated the energy exchange during a fast collision between a spherical stellar system and a perturber of comparable mass, under the assumption that the second-order secular term in the tidal interaction is dominant (see also Alladin 1965). Many authors have treated the problem under the impulsive and the restricted three-body approximations, in which the test stars were assumed to react only to the smoothed-out mass distribution of the galaxy system and the perturber (Contopoulos and Bozis 1964; Sastry and Alladin 1970, 1977; Gallagher and Ostriker 1973; Richstone 1975; Gutowski and Larson 1976). Those approximative calculations were able to estimate the energy exchange and the mass loss, but they were unable to compute detailed mass profile changes.

Richstone (1975) argued that the first order fluctuating term in the tidal interaction dominates for systems in which stellar orbits are more elongated, and found that the fractional change of the tidal radius is equal to the fractional mass loss obtained when fitting to a King model. This result was analytically explained by Knobloch (1978*a*). Knobloch (1978*b*) and Da Costa and Knobloch (1979) solved the Fokker-Planck equation for weak interactions under the impulsive approximation and concluded that—contrary to a suggestion by Layzer (1977)—the effect of the fluctuating term in the tidal force is qualitatively similar to that of the secular term and that relaxed extended envelopes cannot be formed by such mechanism from originally very compact systems.

c) The Present Simulations

The intermediate case of slow hyperbolic encounters, investigated here, closes the gap between very slow and very fast encounters. Such encounters were previously N-body simulated by Bouvier and Janin (1970), Bouvier (1971), Lauberts (1974), and Roos and Norman (1979), but the small N used made it impossible to interpolate any reliable mass profiles. Because of its relevance to the halo-profile problem, we instead concentrate here on the effect of such encounters on the *mass profile*.

We also investigate in detail the mass loss and energy change and identify contributions which, in the impulsive approximation, would have come from the fluctuating and the secular terms of the tidal interaction.

We use a pure N-body code to follow a 250-body spherical system, in which we construct a reliable mass-profile. This system is tidally perturbed by a one- or five-body system of comparable total mass. In order to avoid mergers, we choose the initial orbital parameters for the encounter so as not to satisfy the merger criteria obtained in N-body experiments (van Albada and van Gorkom 1977; White 1978; Roos and Norman 1979) and summarized by Aarseth and Fall (1980, Fig. 1). A necessary condition for a merger to occur in a head-on collision is that the relative velocity at closest approach, v_p, be slower than 1.16 times the escape velocity there, $v_{\rm par}$ (van Albada and van Gorkom 1977). This velocity should be even slower for collisions with larger impact parameters. White (1978) showed that merger occurs in a single crossing time, whenever the slowly colliding systems overlap substantially such that the minimal separation p is smaller than 2.5 times the half-mass radius of each unperturbed system, R_h. We therefore concentrate on collisions with $v_p \geq v_{\rm par}$ and $p \geq 2.5R_h$.

Tidal effects were found to be important whenever the closest approach distance was not larger than $5R_h$ and whenever the encounter was not too hyperbolic. Under such conditions, each "shell" of stars was left, after the collision, with an expanded radius. Gradual stripping occurred outside of $\sim R_h$, steepening the density profile there, while inner parts remained bound. It was found that the net effect on a system which initially had a decreasing $M(R)/R$ profile ($\rho \propto R^{-3}$) is to produce, or extend, an inner region of constant $M(R)/R$ to encompass 50–70% of the bound mass. In the process, about 20–30% of the original bound mass was stripped, and most of it became unbound to either system. A mechanism that produces systems with flat rotation curves over a large fraction of their mass is thus obtained, but which does not produce a relaxed flat outer envelope, in agreement with results of Knobloch (1978*b*) and Da Costa and Knobloch (1979). Tandem encounters of the same system tend to strip the outer parts and produce a smaller system, which retains a flat inner profile.

The results for the energy-gain and the mass-loss were found to be consistent with results derived by the impulsive approximation (even though the encounters were slow) as long as the tidal limit remained valid (i.e., encounters are not too interpenetrating). The "fluctuating term" was shown to be dominant for elongated orbits, while the "secular term" was important for less eccentric orbits.

Our computational method is described in § II. The experiments and the results are given in § III and are compared with previous estimates. In § IV we discuss our results in a cosmological context and apply them to the galactic-halo problem.

II. METHOD

a) *The N-Body Code*

The numerical experiments were based on the N-body code developed and kindly made available to us by Dr. S. J. Aarseth. The code integrates the equations of motion of N softened particles which interact via a potential

$$\phi_{ij} = -Gm_i m_j/[(r_i - r_j)^2 + \epsilon^2]^{1/2}\,, \tag{1}$$

where notations are obvious and ϵ is the softening parameter, which is essential in order to suppress the two-body relaxation effects that arise due to the relatively small number of particles in the experiment. A fourth order polynomial predictor-corrector method is combined with the scheme developed by Ahmad and Cohen (1973) for the separate treatment of the force field due to nearby and to distant particles. A detailed description of the basic N-body may be found elsewhere (Aarseth 1972; Ahmad and Cohen 1973). Two-body relaxation, when a softening parameter is used, is discussed by White (1978; and references therein).

We define our units such that $G = 1$. The softening parameter was chosen to be large enough to ensure that two-body relaxation effects would be negligible through each computer run. We mostly had $\epsilon = 2$, with radius at half-mass, R_h, of ~ 7 units, and total radius of 30–80 units. Integration time steps were chosen so that the range of variation of the total energy of the system over one entire calculation was much less than 1% of its absolute value.

The experiment was run on the CDC Cyber 74 computer of the Hebrew University of Jerusalem, where one crossing time of a typical system lasted about 3 minutes of computer time.

b) *The Unperturbed Configuration*

Particles were initially distributed according to a power-law density profile of the form

$$\begin{aligned} \rho &= \rho_c & (R < R_c) \\ &= \rho_c(R/R_c)^{-\alpha} & (R_c \leq R \leq R_B) \\ &= 0 & (R > R_B)\,, \end{aligned} \tag{2}$$

where $\alpha \simeq 3$ in the cases studied here. The parameters were chosen so that the total mass of the system, M_0, was 270 units. For given α, M_0, and R_h, one parameter, characterizing the "steepness" of the mass profile (R_B/R_c, say), remained free.

A nucleus, containing one-tenth of the total mass, $M_{\rm nuc}$, was represented by a point mass, initially located at the center of mass of the distribution $N_0 = 243$ "stars," of unit mass each, were then distributed around it according to the density profile (2), while their angular location was chosen in random. With the choice of $\epsilon = 2$, the two-body relaxation time was about 30 crossing times of the system, while a typical run lasted about 8–15 crossing times, so that two-body relaxation effects were indeed negligible.

In one case, each star was given, initially, a velocity in a random (isotropic) direction, with magnitude, $V^2(R)$, that ensured local hydrostatic equilibrium:

$$V^2(R) = \frac{3}{\rho(R)}\int_R^{R_B} \frac{M(r)\rho(r)}{r^2}\,dr\,. \tag{3}$$

The initial stellar orbits constructed by this procedure were relatively elongated radially because of the vanishing dispersion velocities on the boundary R_B. In another case, systems with less elongated orbits were constructed. Here each star was still given a velocity according to an equation similar to (3) but in which R_B was replaced by ∞ (where R_B was replaced by ∞, fictitiously, in [2] as well), so that the dispersion velocities did not vanish on the real boundary, $v^2(R_B) \neq 0$. These systems did not begin in hydrostatic equilibrium, but settled to such equilibrium very quickly (see § III*a*).

(Note that the energy truncated King model, commonly used to represent elliptical galaxies in rich clusters [or globular star clusters in galaxies] is not necessarily applicable for dark halos. The assumption of constant nonzero external tidal field is anyway not valid for relatively isolated systems.)

For each initial configuration, the system was also allowed to self-evolve for 20 crossing times or more. The resultant shapes were then used as references to compare to the perturbed cases following the same number of crossing times.

c) *Tidal Encounters*

A perturber of mass $M_p = nM_0$ ($n = 1, 2$) was represented by N_p particles ($N_p = 1$ or 5) which, for $N_p = 5$, were distributed randomly within a given sphere of radius 6. The main reason for using, in some cases, a five-body perturber instead of a single-body perturber was technical, to suppress accumulated numerical errors. (A way to overcome this problem has since been shown by S. J. Aarseth.) The perturber center of mass, with a relative velocity v_0 and an impact parameter b_0, was initially located at a distance of $r_0 = 100$ units ($\sim 15R_h$) from the center of mass of the perturbed system. In most cases, the parameters were chosen such that the relative velocity at infinity, v_∞, was positive, and the closest approach distance, p, was larger than $2R_h$. The initial conditions were set, as described previously, to simulate close slow hyperbolic tidal encounters where mergers did not occur.

Encounters were followed, in the center-of-mass frame, until the separation grew to values much larger than r_0. At given stages of the encounters, usually separated by time intervals equal to the crossing time of the unperturbed system, the system was scanned to record the mass loss, energy exchange, and the mass profile.

Note that one does not expect *a priori* that the impulsive approximation will be valid for these simulations.

d) *Mass Loss and Energy Change*

At each stage, the center of mass of the N_0 particles was computed. Then, all stars with positive energy relative to that center of mass were identified as escapers, and the center of mass of the N_b remaining bound stars was evaluated. The escapers relative to this new center of mass were identified next, and this iterative procedure continued until convergence was reached. The final values for the escaped mass, ΔM, and the center of mass of the remaining bound system, of mass M_b, were recorded. The final fractional mass loss, $\Delta M/M_0$, is one number in which we were interested.

The internal energy of a system of particles is the sum of the kinetic energies of the particles relative to their center of mass, $\boldsymbol{R}_{\rm cm}$, and their mutual gravitational interaction energy, namely,

$$E = \sum_i \tfrac{1}{2} m_i (\dot{\boldsymbol{r}}_i - \dot{\boldsymbol{R}}_{\rm cm})^2 - \tfrac{1}{2} \sum_i \sum_j m_i m_j / [(\boldsymbol{r}_i - \boldsymbol{r}_j)^2 + \epsilon^2]^{1/2} \,. \tag{4}$$

At each stage, we calculated it twice: first for the bound system, to find E_b, and then for the perturbed system as a whole (including the escapers), to find E_t. The change in internal energy of the perturbed system, ΔE_t, and in that of the perturber (whenever $N_p > 1$) is at the expense of the relative energy of the two-body system. Here we were interested in the final fractional energy changes, $\Delta E_b/E_0$ and $\Delta E_t/E_0$, where E_0 is the internal energy of the unperturbed system.

e) *Mass Profile and "Rotation Curve"*

Three different methods were tried in order to determine the "effective center" relative to which the spherical mass profile was to be calculated: (1) the center of mass of the bound system or of an inner part, (2) the central massive nucleus itself, and (3) the center of a sphere, of some given radius s, which was moved in the distribution until it encompassed the maximum mass. Two values of s were tried: (a) the radius of half the bound mass distribution and (b) the radius of about 0.2 of that distribution.

All methods gave similar results but method 3a seems to be the best in most cases, since radii containing given fractions of the bound mass tended to be the smallest when evaluated by this method. Therefore, method 3a was chosen to define the "effective center" of the bound system.

The radii of spheres around the effective center containing 0.15, 0.20, 0.25, ..., 0.95, 1.00 of the bound mass M_b were then evaluated in order to find the mass profile. A smooth mass profile was obtained by averaging over three successive time stages (separated by a crossing time or half of it), such that temporal features and local oscillations were averaged out. Those small-period changes were used to estimate the error about the average value.

Since our main interest here was the mass-profile in dark halos, we obtained an average "rotation curve" by averaging $M(R)/R$, in units of each current M_b/R_h value. A density profile was also obtained, on dividing the mass of shells containing one-tenth of the total bound mass by the volumes they occupy, and again averaging over three successive time stages.

Note that we do not expect significant results for core densities, both because we have represented part of the core by a massive body and because of the large softening parameter used (two-body relaxation effects would otherwise be important there).

III. EXPERIMENTS AND RESULTS

a) *Unperturbed Models*

Two different initial configurations, which we denote by A and B, were used and their characteristic parameters are given in Table 1. According to the choice of the initial velocity profile (see § IIb), the envelope of model A consists of elongated stellar orbits, typical of systems formed via collapse, while model B consists of less eccentric orbits. The mean elongation of the orbits in each envelope could be illustrated by the ratio of radial and tangential velocity dispersion, σ_r^2/σ_t^2, in the outer 30% of the mass, say. This ratio is around 0.3 in model B and is about 1 in model A, after it has relaxed to hydrostatic equilibrium. The unperturbed profiles of models A and B after 15 crossing times are shown in Figure 1. The systems have actually relaxed in a couple of crossing times into equilibrium shapes which were quite similar to the initial ones. No signs of two-body relaxation effects were found until more than 20 crossing times had elapsed.

Although both cases have density profiles in which most of the mass follows the $\rho(R) \propto R^{-3}$ power law, their

TABLE 1
STARTING MODELS

Model	R_c	R_B	E_o	v_{rms}	t_D	R_h	R_{rms}	σ_r^2/σ_t^2
A....................	0.8	89.5	−2143	4.0	4.27	(7.2) 6.5	26	1.0
B....................	2.0	20.0	−2243	4.1	4.00	(5.8) 6.5	13	0.3

NOTE.—The models are characterized by R_c and R_B, the core and the boundary radii. E_o is the internal energy, v_{rms} is the mean dispersion velocity, and t_D is the dynamical (≡ crossing) time of the system. The final values of R_h (half-mass radius) and R_{rms}, are given at $t = 15t_D$, while starting values are given in brackets. The quantity σ_r^2/σ_t^2 is the mean ratio between the radial and tangential velocity dispersion in the outer 30% of the mass, in equilibrium. Both models have $\alpha = 3$, $M_o = 270$, $M_{nuc} = 27$, and $\epsilon = 2$ (see § II). All quantities are expressed in the experiment units.

mass profiles are different because of their different core radii. Model A has only a small fraction of its mass (less than one-third) in a region where $M(R)/R$ might be regarded as constant while in most of its parts $M(R)/R$ drops rapidly with R; model B represents a system which already has a flat $M(R)/R$ up to its half-mass radius. One might consider model A to qualitatively represent initial halos or their subsystems, formed by collapse or by violent mergers, while model B might represent a stage in the evolution of a halo towards is final shape, or perhaps the final configuration itself.

b) Encounters

Encounters were simulated between systems of type A or B and a perturber. The parameters characterizing the encounters, denoted by A1, A2, ..., and B1, B2, ..., respectively, are given in Table 2.

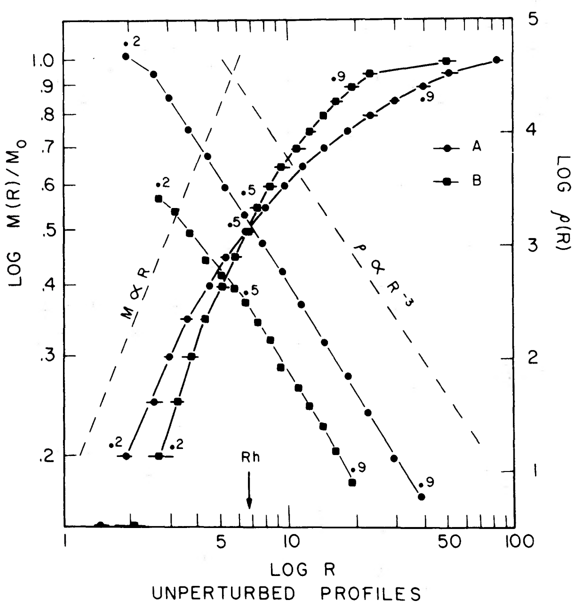

FIG. 1.—The unperturbed profiles. The mass-profiles, in fractional units, and the density profiles, in arbitrary units, of the unperturbed models A and B after 15 crossing times. The radius R is given in the experiment absolute units, and the radius of the half-mass is indicated by R_h. The various dots correspond to 0.2, 0.25, ..., 0.9 of the total mass, and the curves are free-hand interpolations.

The perturber was mostly equal in mass to the perturbed system or twice as massive. In one case it had a mass of 10 M_0. The closest approach distances p, were varied from 5.75 R_h in distant encounters down to head-on collisions. The relative velocities at closest approach v_p, were slightly above the parabolic velocity in most cases, to avoid mergers, but some faster collisions were simulated as well. Tandem encounters, with the same initial conditions, were simulated in some cases and are denoted by *a*, *b*, and *c*. A7 is an example of a continuous tidal encounter in a circular orbit. Results for the mass loss, energy change, and the half-mass radius change are also given in Table 2.

Figure 2 illustrates typical encounters, where the general effects of tidal interaction on the mass distribution of the system might be seen in certain stages along the encounter.

c) Mass Loss and Energy Change

The fractional mass loss, $\Delta M/M_0$, the fractional change of the internal energy of the bound system, $\Delta E_b/E_0$, and the fractional change of the energy of the original system as a whole (including the escapers), $\Delta E_t/E_0$ were obtained for each encounter at some final time t, when the separation is r, and are given in Table 2. As was expected, there was a significant mass loss from the system—especially in the A-cases. However, unlike previous numerical results (Lauberts 1974; Richstone 1975), there was a positive energy gain in the bound system in all cases studied here.

It might be of general interest to investigate the dependence of the results on the encounter parameters for the different models A and B, and to compare it with previous theoretical and numerical estimates.

i) The Impulsive Approximation—Fluctuating and Secular Terms

The basic theory is due to Spitzer (1958). Under the impulsive approximation, i.e., on assuming that the stars do not move appreciably as the perturber passes by, the energy transfer to a test star in a tidal encounter, ΔE_*, is just

$$\Delta E_* = m_* V_* \cdot \Delta V_* + m_*(\Delta V_*)^2/2 , \qquad (5)$$

where V_* is the velocity of the star and ΔV_* is its increment. Obviously, equation (5) contains a "first-

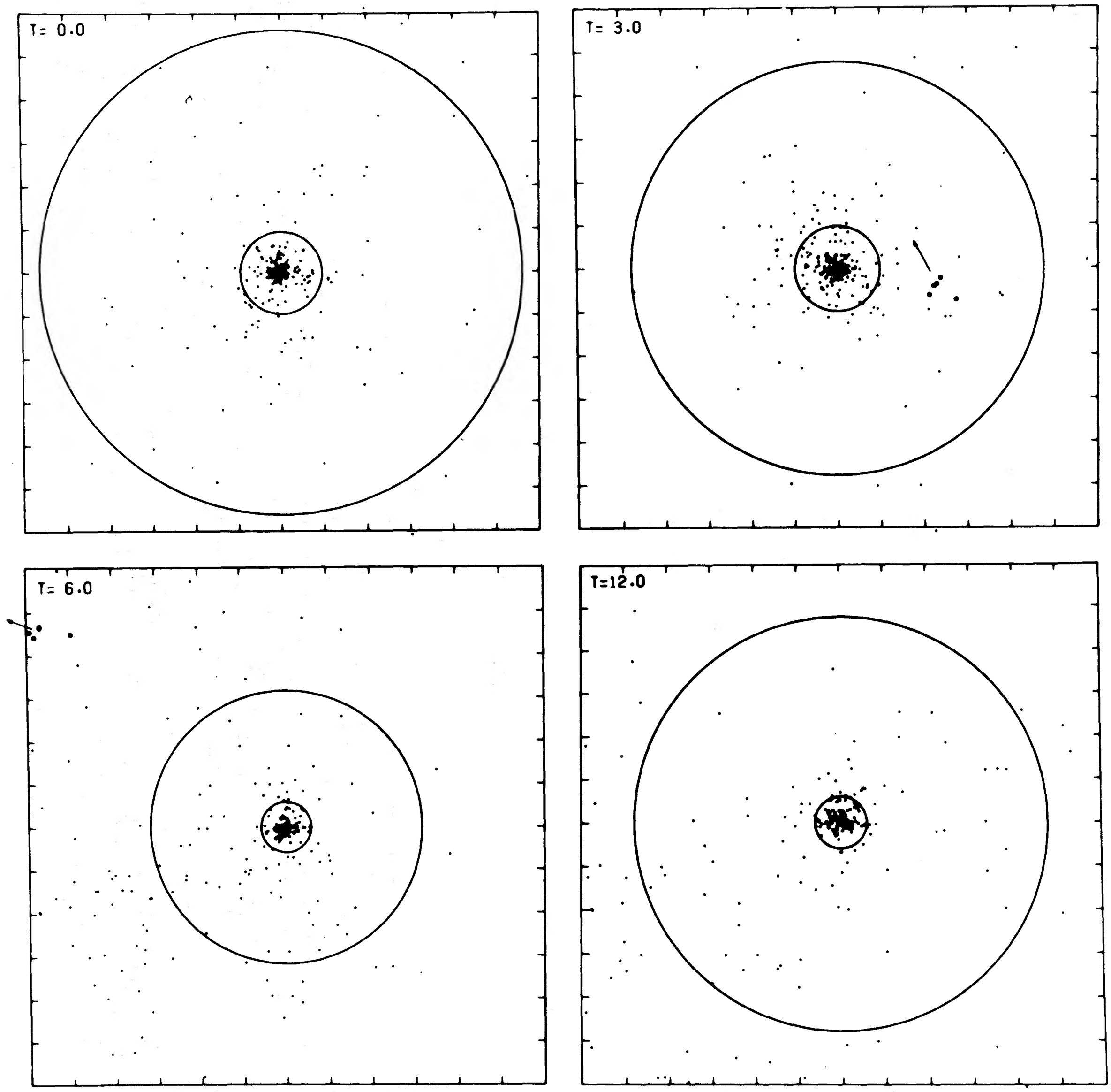

FIG. 2*a*

FIG. 2.—(*a*, *b*) Projections of the system on the plane of the encounter, shown at certain stages during the encounter. Time is given in units of the crossing-times. Dots represent the particles of the perturbed system, while the particles of the perturber are denoted by larger symbols. Circles of radii corresponding to 50% and 90% of the bound mass are plotted around the "effective center" (see § II*e*). The marks on the axes are separated by 10 units. (*a*) Model A3, a typical slow tidal encounter. (*b*) Model B7, a head-on, fast collision.

order," fluctuating term and a "second-order," secular term.

On averaging over the stars, the fractional energy change of the stellar system becomes

$$\frac{\Delta E}{E} = \frac{2\langle V_* \cdot \Delta V_* \rangle}{V_{\rm rms}^2} + \frac{(\Delta V_*)_{\rm rms}^2}{V_{\rm rms}^2}$$
$$= g\frac{(\Delta V)_{\rm rms}}{V_{\rm rms}} + \frac{(\Delta V)_{\rm rms}^2}{V_{\rm rms}^2}, \quad (6)$$

where g is a numerical factor determined by the distribution function of the stellar system alone (as long as the average eccentricities of the stellar orbits are only weakly dependent on the radius; otherwise, g depends on the encounter parameters). For a stellar system in equilibrium, g is expected to vanish due to the symmetry between stars that "go out" and "come in" at any given point.

In the tidal limit, the rms velocity increment can be approximated by (Spitzer 1958)

$$(\Delta V)_{\rm rms} = \frac{2GM_p}{p^2 v_p} (\tfrac{2}{3})^{1/2} R_{\rm rms}, \quad (7)$$

where M_p is the mass of the perturber, p and v_p are the

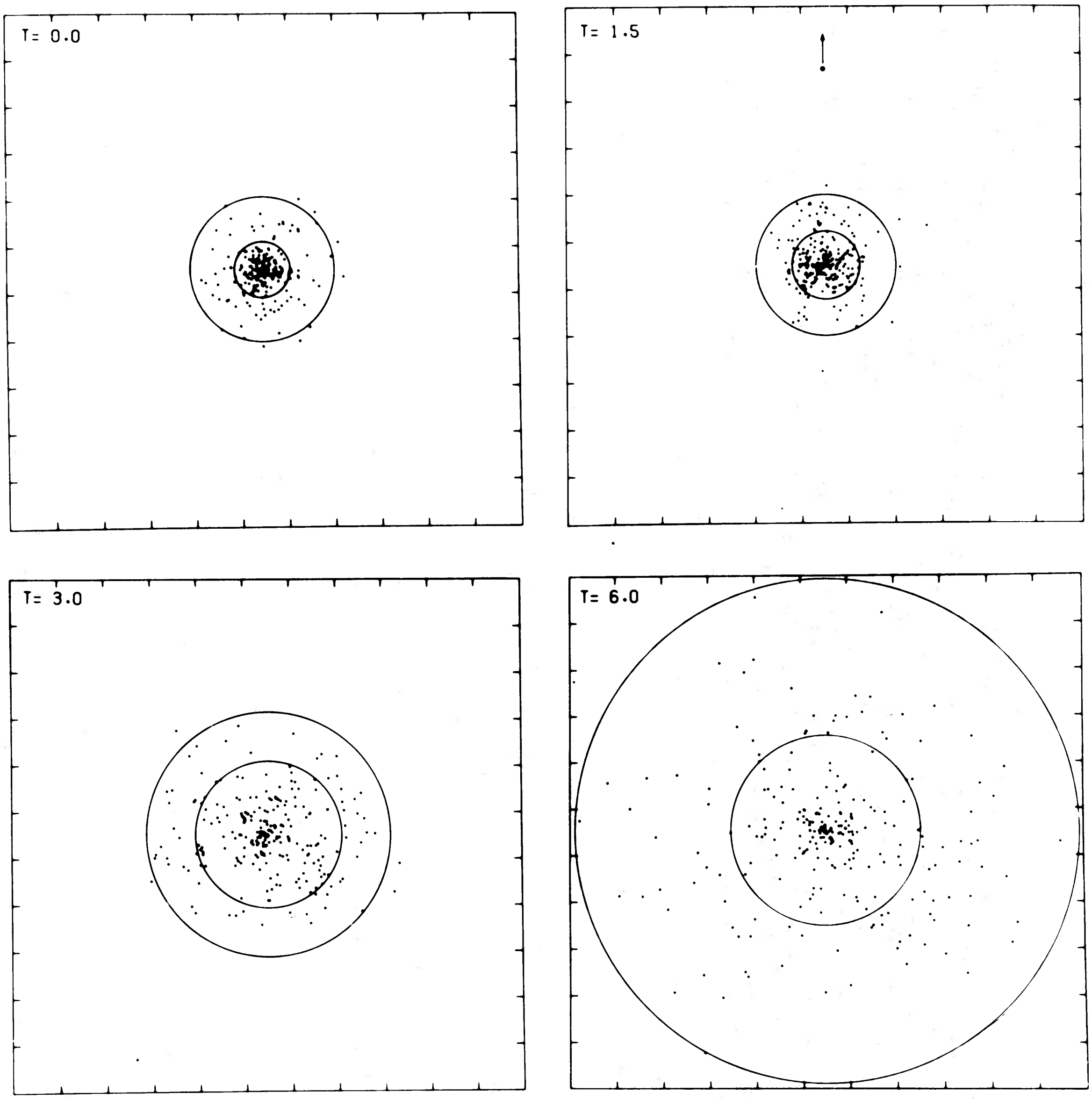

FIG. 2*b*

minimal separation and the relative velocity there, and $R_{\rm rms}$ is the rms radius of the stellar system. We therefore choose the dimensionless parameter

$$\nu_{\rm tidal} \equiv \frac{(\Delta v)_{\rm rms}}{v_{\rm rms}}(\text{tidal limit}) \equiv \frac{2GM_p}{p^2 v_p}\left(\tfrac{2}{3}\right)^{1/2}\frac{R_{\rm rms}}{v_{\rm rms}} \quad (8)$$

to characterize the encounter in the tidal limit.

Spitzer (1958) assumed that the fluctuating term is averaged out so that the secular term is dominant, while Richstone (1975) argued that there may be cases in which the first-order term rather dominates the evolution: when only those stars escape for which $\mathbf{v}_* \cdot \Delta \boldsymbol{v}_*$ is positive, the stars which remain bound make a negative net contribution to the first-order term. Such a situation may arise when the stellar orbits tend to be radial, such that for many stars $\boldsymbol{v}_* \| \Delta \boldsymbol{v}_*$, where $\Delta \boldsymbol{v}^*$ is directed toward the point of closest approach (cf. Gallagher and Ostriker 1972).

ii) *Dependence on the Encounter Parameter*

In Figure 3 we plot the fractional energy gain and the fractional mass loss as a function of $\nu_{\rm tidal}$. Figure 3*a* shows that for the A-model, which consists of elongated orbits, the general dependence is linear,

$$-2\frac{\Delta M}{M} \approx -2\frac{\Delta E_b}{E} = -\frac{\Delta E_t}{E} \approx \nu_{\rm tidal} \,. \quad (9)$$

Figure 3*b* shows that for the B-model, which consists of less elongated stellar orbits, the dependence is parabolic:

$$-\frac{9}{2}\frac{\Delta M}{M} \approx -\frac{3}{2}\frac{\Delta E_b}{E} \approx -\frac{\Delta E_t}{E} \approx {\nu_{\rm tidal}}^2 \,, \quad (10)$$

1980ApJ...241..946D

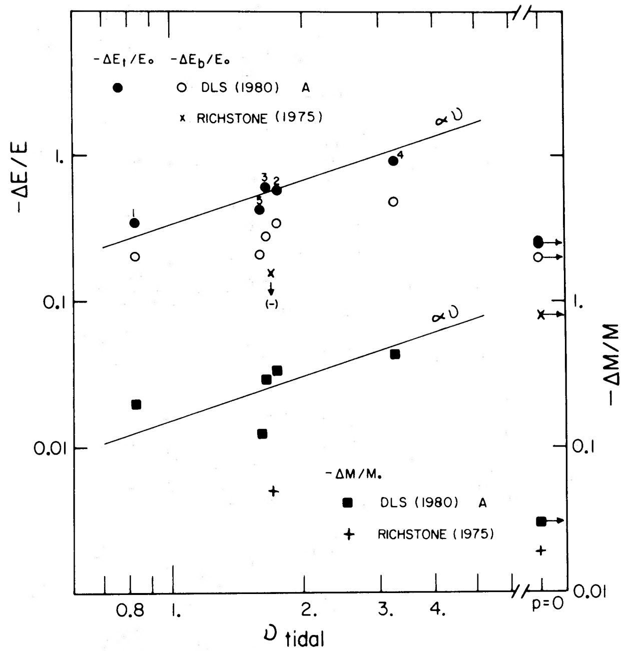

FIG. 3*a*

FIG. 3.—(*a, b*) Energy gain and mass loss. Our results (DLS) for the fractional mass loss, $\Delta M/M_0$, the fractional energy gain to the bound system, $\Delta E_b/E_0$, and the fractional energy change which includes the escapers, $\Delta E_t/E_0$, are plotted as functions of the impulsive-approximation parameter in the tidal limit $\nu_{\rm tidal} \equiv (2GM_p/p^2 v_p)(\frac{8}{3})^{1/2}(R_{\rm rms}/v_{\rm rms})$. The model indices are indicated. Previous estimates are also shown. The mass-loss scale is shifted down by a factor of 10. Minus signs $(-)$ denote negative values. (*a*) A-models. The line shows the expected linear dependence on $\nu_{\rm tidal}$ when the first-order fluctuating-term of the tidal interaction is dominant (highly eccentric stellar orbits). (*b*) B-models. The lines show the expected dependence on $\nu_{\rm tidal}{}^2$ when the second order fluctuating term is dominant (low-eccentricity stellar orbits). The upper line is $-\Delta E_t/E_0 = \nu_{\rm tidal}{}^2$ as was analytically estimated by Spitzer (1958). The deviations from the power law dependence, which show up in some cases of $\nu_{\rm tidal} > 0.5$, correspond all to interpenetrating collisions ($p \leq 2R_h$).

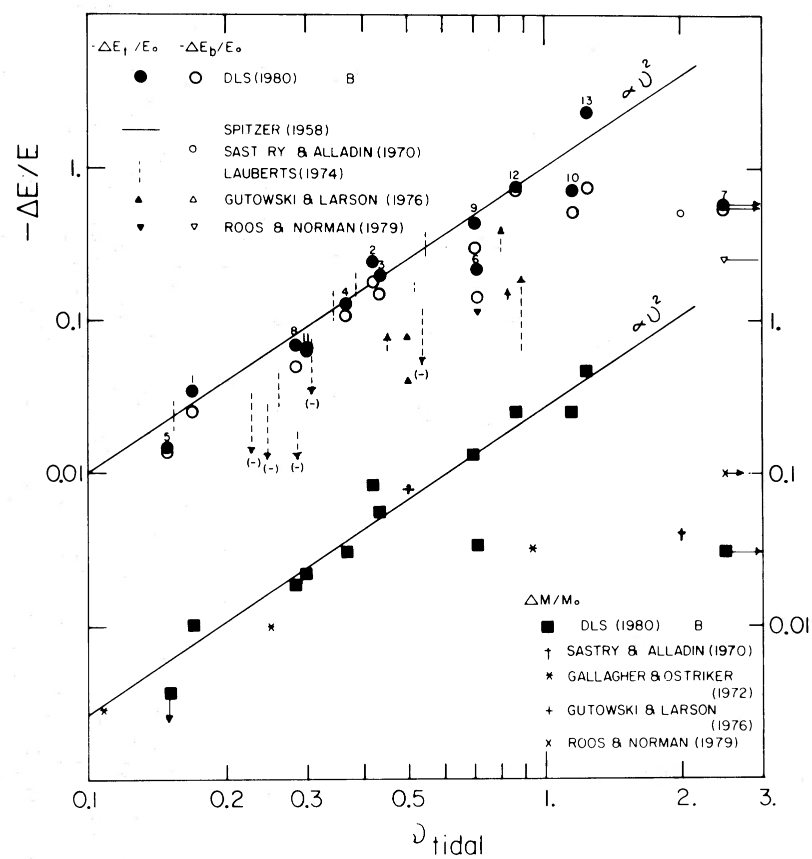

FIG. 3*b*

TABLE 2

ENCOUNTER PARAMETERS AND RESULTS

Model	Initial: $\frac{M_p}{M_o}$	Initial: N_p	Initial: $\frac{b_o}{R_h}$	Initial: $\frac{v_o}{v_{rms}}$	Closest Approach: $\frac{p}{R_h}$	Closest Approach: $\frac{v_p}{r_{qms}}$	Closest Approach: $\frac{v_p}{v_{par}}$	Closest Approach: v_{tidal}	Final: $\frac{t}{t_p}$	Final: $\frac{r}{R_h}$	Final: $-\frac{\Delta M}{M_o}$ ($\pm$.004)	Final: $-\frac{\Delta E_b}{E_o}$ ($\pm$.01)	Final: $-\frac{\Delta E_t}{E_o}$ ($\pm$.01)	Final: $-\frac{\Delta R_h}{R_{ho}}$ ($\pm$.05)
A1	2	5	7.69	1.15	4.62	1.92	1.04	0.83	15	24.6	0.22	0.20	0.36	0.19
			(15.90)	(0.56)										
A2	2	5	5.54	1.25	2.80	2.47	1.05	1.75	15	8.20	0.33	0.33	0.58	0.37
			(9.32)	(0.74)										
A3	2	5	4.80	1.53	2.80	2.63	1.11	1.65	15	36.2	0.29	0.28	0.59	0.33
			(6.38)	(1.15)										
A4	2	5	3.66	1.58	1.82	3.16	1.33	3.24	8	18.2	0.39	0.47	0.91	0.37
			(4.76)	(1.21)										
A5	1	5	2.59	2.22	1.82	3.16	1.33	1.62	8	30.6	0.12	0.21	0.42	−0.01
			(2.79)	(2.07)										
A6	1	5	0.	5.75	0.	6.42	2.16	head-on	7	89.4	0.048	0.20	0.26	−0.20
			(0.)	(5.69)										
A7	1	5	7.69	0.82		circular			25	6.15	0.14	0.28	0.28	0.17
B1	1	1	7.58	1.12	5.50	1.55	1.16	0.17	10	19.4	0.010	0.026	0.035	0.06
			(10.82)	(0.78)										
B2	1	1	9.55	0.57	3.45	1.58	0.94	0.42	19	13.6	0.085	0.18	0.25	0.02
B3a	1	1	5.30	1.12	3.05	1.95	1.09	0.44	10	18.9	0.055	0.15	0.20	0.05
			(10.36)	(0.78)										
B3b			tandem		3.14	1.97	1.10	...	11.4	19.8	0.19	0.33	...	0.11
					(2.90)	(2.03)			(8)	(18.3)	(0.14)	(0.21)		(0.06)
B3c			tandem		3.27	1.89	1.12	...	12.1	22.3	0.30	0.41	...	0.25
					(3.34)	(2.04)			(6)	(26.9)	(0.14)	(2.12)		(0.16)
B4	1	1	4.09	1.76	3.01	2.39	1.33	0.37	10	36.2	0.030	0.11	0.13	−0.07
			(5.00)	(1.56)										
B5	1	1	3.12	5.61	3.01	5.84	3.24	0.15	4	40.8	0.004	0.023	0.023	0.10
			(3.15)	(5.55)										
B6	1	1	1.53	5.26	1.38	5.84	2.20	0.72	5	56.4	0.033	0.14	0.22	−0.04
			(1.55)	(5.20)										
B7	1	1	0.	5.61	0.00	6.29	2.12	head-on	4	40.3	0.030	0.56	0.56	−1.42
			(0.)	(5.55)										

TABLE 2—*Continued*

Model	Initial: $\frac{M_p}{M_o}$	Initial: N_p	Initial: $\frac{b_o}{R_h}$	Initial: $\frac{v_o}{v_{rms}}$	Closest Approach: $\frac{p}{R_h}$	Closest Approach: $\frac{v_p}{r_{qms}}$	Closest Approach: $\frac{v_p}{v_{par}}$	Closest Approach: ν_{tidal}	Final: $\frac{t}{t_p}$	Final: $\frac{r}{R_h}$	Final: $-\frac{\Delta M}{M_o}$ $(\pm.004)$	Final: $-\frac{\Delta E_b}{E_o}$ $(\pm.01)$	Final: $-\frac{\Delta E_t}{E_o}$ $(\pm.01)$	Final: $-\frac{\Delta R_h}{R_{ho}}$ $(\pm.05)$
B8	2	1	8.64	1.12	5.75	1.69	1.06	0.28	10	18.8	0.018	0.050	0.070	0.06
			(17.80)	(0.54)										
B9a	2	1	6.29	1.12	3.19	2.21	1.03	0.71	10	18.9	0.13	0.30	0.44	0.02
			(13.00)	(0.54)										
B9b			tandem		3.56	2.07	1.06	...	11.5	19.1	0.38	0.54	...	0.21
					(3.31)	(1.90)			(6)	(17.7)	(0.29)	(0.34)		(0.19)
B10	2	1	5.30	1.12	2.31	2.58	1.03	1.15	9	15.9	0.25	0.53	0.74	−0.04
			(10.90)	(0.54)										
B11	2	1	3.20	5.50	3.01	5.84	2.65	0.30	4	45.4	0.022	0.065	0.065	0.06
			(3.25)	(5.40)										
B12	2	5	5.45	1.22	2.75	2.41	1.05	0.87	15	20.3	0.26	0.45	0.75	0.20
			(9.18)	(0.72)										
B13	10	1	12.5	1.12	4.56	3.07	0.90	1.25	7	11.7	0.45	0.75	2.31	0.08

NOTE.—M_p and N_p are the mass and number of heavy particles in the perturber. b_o and v_o are the initial impact parameter and relative orbital velocity at the initial separation $d_o = 100$, while the same quantities at infinity, for hyperbolic encounters, are given in brackets beneath. The quantities p and v_p are the closest approach distance and the orbital velocity there, given also in units of the parabolic velocity there. The encounters are characterized in the tidal limit by the parameter $\nu_{tidal} \equiv (2GM_p/p^2 v_p)(8/3)^{1/2}(R_{rms}/v_{rms})$. The results are obtained at the final time t in which the separation is r. $\Delta M/M_o$ is the fractional mass loss, $\Delta E_b/E_o$ and $\Delta E_t/E_o$ are the fractional internal energy change of the remnant bound system and of the original system as a whole, including the escapers. $\Delta R_h/R_{ho}$ is the fractional change of the half-mass-radius of the bound mass. The values in brackets for the tandem encounters are expressed in units of the updated R_h, v_{rms}, and t_D of the remnant system which would undergo another encounter.

in good agreement with the results of Spitzer (1958).

The only deviations from (9) or (10) are due to interpenetrating collisions (such as B6, B10, and A5). In these cases, the tidal limit is probably not valid, and one should take into account the direct effect of the perturber on the stars. It was shown by Richstone (1975) that in this case the velocity increment in the impulsive approximation is

$$(\Delta v)_{\rm rms} \propto GM_p/pv_p \tag{11}$$

so that another parameter, $v_{\rm direct} \propto (pv_p)^{-1}$, should replace $v_{\rm tidal}$ in characterizing the encounters.

The head-on collisions show a low rate of mass loss. We find for fast collisions in the A-model

$$-7\frac{\Delta M}{M} \approx -2\frac{\Delta E_h}{E} \approx -\frac{\Delta E_t}{E_t}, \tag{12}$$

while in the B-model

$$-30\frac{\Delta M}{M} \approx -1.5\frac{\Delta E_b}{E} \approx -\frac{\Delta E_t}{E}. \tag{13}$$

It is clear from (9), (10), (12), and (13) that the mass loss per energy gain unit is smaller for the B-model, which means that it is harder to tear up a star from the B-model. This is consistent both with the fact that in the B-model the outer stars are more tightly bound and with the action of the weaker, second order secular effect there.

iii) *Escaping Trajectories*

The difference in character between our models A and B, which was manifested in Figure 3 and was discussed above, becomes even sharper on considering the escapers. This is shown in Figure 4 for two typical cases in the perturbed system frame. In model A3 (Fig. 4*a*) very few escapers are bound to the perturber; most of the escaping stars run away in a direction which is opposite to the closest approach direction. By contrast, in model B9a (Fig. 4*b*), a large fraction of the escapers become bound to the perturber while the rest escape in various directions.

That A-cases have a preferred escape direction is consistent, in the impulsive approximation, with the strong first-order effect: stars on radial orbits parallel to the closest approach direction gain the maximal $\boldsymbol{v}\cdot\Delta\boldsymbol{v}$ contribution and escape in hyperbolic orbits to the opposite direction. They do not tend to become bound to the perturber because their velocities are radial, hence perpendicular to the velocity of the perturber at closest approach.

In the B-cases, many stars are in orbits which are qualitatively circular so that, in the impulsive approximation, the fluctuating term is negligible ($\boldsymbol{v}\cdot\Delta\boldsymbol{v} \approx 0$) and the stars which are mostly affected by the second order term are those near the perturber. Many of them become naturally bound to the perturber because their velocities might be tangent to its trajectory to begin with, and they thus feel its attraction for a long time.

iv) *On the Relation with the Impulsive Approximation*

There is no *a priori* justification for applying the simple arguments based on the impulsive approximation in most of the cases studied here; although the energy exchange occurs mostly during less than one crossing time around the time of closest approach, it certainly does not happen instantaneously. However, our simulations show that the dependence of the energy exchange (and of the mass-loss) on $v_{\rm tidal}$ is consistent, in the tidal limit, with the results

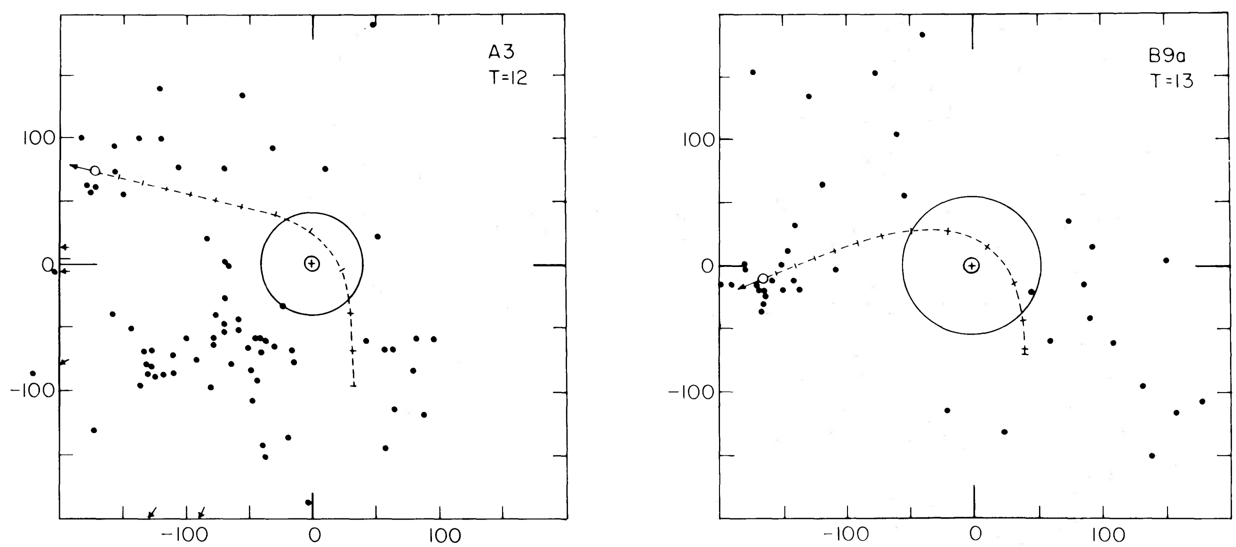

FIG. 4*a* FIG. 4*b*

FIG. 4.—(*a*, *b*) Distribution of escapers. A snapshot of the spatial distribution of the escaped stars as projected on the encounter plane after the encounter. Each dot denotes an escaper. The perturber is denoted by a circle, and its trajectory in the effective-center-frame of the perturbed system is shown. The concentric circles denote the half-mass-radius and the 90%-mass-radius of the remnant bound system. (*a*) A-model. Most the stars escape in a preferred direction which is opposite to the perihelion of the encounter. About 10% of the escapers became bound to the perturber. Small arrows indicate stars which are already out of the figure frame. (*b*) B-model. About 40% of the escapers became bound to the perturber.

predicted by the impulsive approximation. The dependence on the mean elongation of the stellar orbits is also consistent with this simple theory.

If we try to formally push further the validity of the impulsive approximation in our cases, the *positive* internal energy gain that was found in the A cases might be somewhat puzzling, because the "first-order term" in $v_{\rm tidal}$ is dominant there (§§ III*c* [ii] and III*c* [iii]). In the impulsive approximation, this would indicate that $\langle \boldsymbol{v} \cdot \Delta \boldsymbol{v} \rangle$ is positive when averaged over the stars of the perturbed system during the collision. It seems that when the tidal forces are maximal, there is already an induced (zero-order) expansion of part of the system so that in the neighborhood of the perturber, stars effectively move outward (they also move that way in a symmetric region on the opposite side of the system.)

A possible reason for such expansion might be that the central attractive forces, which are acting on stars, weaken due to the "cigar" shape of the system, which was tidally induced during earlier stages of the encounter. (A similar effect had been recognized in connection with escaping stars from collapsing globular clusters [Hénon 1964] as was pointed out to us by D. Lynden Bell.) However, the case should be studied in more detail before a simple, conclusive interpretation can be given.

v) *Comparison with Previous Results*

At any rate, an important conclusion of our simulations is that results derived on using the impulsive approximation remain valid, in the tidal limit, for both radial and circular orbits. The pioneering analytic estimates of Spitzer (1958) for the second-order effects in $v_{\rm tidal}$ are found to be exact for our B-models, both in magnitude and in functional dependence on the encounter parameters, while Richstone's (1975) arguments for the contribution of the first-order term are found to be qualitatively valid in our A-models.

Most previous numerical investigations have dealt with stellar systems which had circular orbits. Their results should therefore be compared with our results for model B, and some of them are shown in Figure 3*b*.

Sastry and Alladin (1970) report results of deeply interpenetrating collisions between two identical spherical systems represented by $n = 4$ polytropes; their results are indeed in good agreement with ours for head-on collisions (B7).

The results of Roos and Norman (1979), obtained by *N*-body simulations with 28 particles (94 in some cases), overestimate our results for the mass loss in the head-on collisions (by at least a factor of 2) and underestimate the energy gain results. They also find $(\Delta M/M)/(\Delta E_b/E) \approx 0.45 \pm 0.2$, in disagreement with our result (13). This is likely to be due to the fact that they look at two identical colliding systems while we represent the perturber as a single body, an effect which should indeed be important for head-on collisions (see III*e* below). However, they still find a dependence on v_p^{-2}, showing the importance of the second-order term in this case. Their results for interpenetrating, non–head-on, collisions are in better agreement with ours; they find $(\Delta M/M)/(\Delta E_b/E) = 0.7 \pm 0.4$ which is consistent with (10).

Gutowski and Larson (1976), who simulated an interpenetrating parabolic encounter with a smaller companion in the restricted three-body approximation, give results which are in good agreement with ours.

Gallagher and Ostriker (1972) checked the mass-loss due to fast encounters with a massive perturber under the impulsive approximation, and under the assumption that the perturber is only slightly deflected from a straight-line trajectory. They report a strong dependence on v_∞, again consistent with the secular term. They investigate very rapid collisions, and their results for the slowest cases are in good agreement with our most rapid ones, for several values of closest approach distance (cf. our cases B5 and B6 in comparison with their results for $v = 1500$ km s^{-1}).

The *N*-body experiments of Lauberts (1974), simulating slow encounters between two identical 16-body systems, are in good agreement with our results for the energy change. They deviate from the $v_{\rm tidal}{}^2$ line when collisions are too interpenetrating, just as we found, or when the encounters are more distant than in the cases we study. In such cases he finds possible small energy losses from the system, but the error in his results is very large (mostly due to the small number of particles he uses).

It is hardly surprising that Richstone (1975), who simulated fast collisions under the restricted three body and the impulsive approximations, finds most of the results reported previously to be inconsistent with his own. As was suggested by him, this was clearly due to the fact that his test system was represented by a King model in which many elongated orbits were present, in contrast with the situation in the other works. We have shown that the character of the orbits in the test system decisively influences the changes it undergoes in a tidal encounter. Therefore, his results should be compared with our A-model where the first order term is dominant, and indeed, he finds that escaping orbits are in a preferred direction. He finds that the mass loss is indeed proportional to $v_\infty{}^{-1}$, in agreement with our results and with the fluctuating term in the impulsive approximation, and that the dependence on the impact parameter is even weaker than p^{-1}, which is probably due to the invalidity of the tidal limit in his interpenetrating collisions. The peak he finds in $\Delta M/M$ at $p \approx R_h$ is in agreement with our results. However, we still find some discrepancies; Richstone finds the energy changes to be more complicated than what is predicted by the impulsive approximation and not proportional to the mass loss. He underestimates them both by a factor of ~ 2 in most cases and also finds, in some cases of slow encounters, energy losses from the system which are in disagreement with our results (see Fig. 3*a*). This might be due to his refitting to a King model after the collision, a procedure which might artifically affect the results.

d) *Mass Profiles*

i) *Results*

The resultant mass profile of the bound system in each model is evaluated at some postencounter time whose

TABLE 3

MASS PROFILES

M/M_b	A	A1	A2	A3	A4	A5	A6	A7
0.2	0.30	0.35	0.34	0.37	0.38	0.35	0.40	0.34
0.3	0.46	0.59	0.65	0.55	0.61	0.53	0.57	0.51
0.4	0.69	0.74	0.83	0.75	0.81	0.71	0.74	0.71
0.5	1.00	1.00	1.00	1.00	1.00	1.00	1.00	1.00
0.6	1.48	1.27	1.22	1.40	1.42	1.58	1.61	1.46
0.7	2.21	1.78	1.72	2.01	2.31	2.91	3.18	2.32
0.8	3.54	2.68	2.96	3.19	6.18	4.77	4.88	5.02
0.9	6.00	8.18	10.51	8.86	10.17	6.97	6.60	9.50
1.0	12.71	18.76	18.69	22.06	14.84	9.06	11.20	15.34
R_h	6.5	5.23	4.09	4.32	4.08	6.55	7.82	5.37
$-\Delta M/M_0$	...	0.22	0.33	0.29	0.39	0.12	0.048	0.14

M/M_b	B	B1	B3c	B7	B8	B9a	B9b	B10
0.2	0.42	0.48	0.44	0.36	0.44	0.40	0.37	0.43
0.3	0.58	0.68	0.67	0.58	0.65	0.59	0.61	0.61
0.4	0.77	0.85	0.82	0.76	0.81	0.78	0.85	0.78
0.5	1.00	1.00	1.00	1.00	1.00	1.00	1.00	1.00
0.6	1.32	1.34	1.27	1.53	1.31	1.36	1.22	1.38
0.7	1.68	1.72	1.60	2.33	1.80	1.92	1.53	2.15
0.8	2.14	2.39	2.50	3.00	2.33	3.46	2.36	3.86
0.9	3.04	3.46	5.80	4.06	3.70	7.72	7.42	7.82
1.0	7.94	7.96	13.65	5.83	12.33	13.39	12.40	10.78
R_h	7.15	6.75	5.38	17.27	6.76	7.02	5.63	7.44
$-\Delta M/M_0$	...	0.010	0.30	0.033	0.018	0.13	0.38	0.25

NOTE.—The radii 0.2, 0.3, ..., 1 of the bound mass are given in units of its half-mass radius for several models. The unperturbed profiles for A and B are evaluated at $t = 15t_D$ and at $t = 10t_D$, respectively. R_h is given in the units of the experiment, and the fractional mass loss, $\Delta M/M_0$, is also indicated.

value is given in Table 2. "Relative" profiles are given in Table 3, in which the radii of some fractions of the bound mass are given in units of its half-mass-radius. "Absolute" mass profiles of typical cases of types A and B are plotted in Figure 5, where the masses and the radii are measured in fixed units. The corresponding "relative" $M(R)/R$ profiles, which might indicate "rotation curves," are shown in Figure 6.

ii) *The Outer Envelope*

In general, each "shell" of stars settles at a radius which is larger than its original one: stars are preferentially stripped from regions outside R_h regions while inner stars remain bound. The density profile in the outer parts thus becomes steeper rather than forming a relaxed extended envelope. A similar result has been obtained by Knobloch (1978*b*) and by Da Costa and Knobloch (1979) for *weak* (distant and fast) tidal interactions on making use of the impulsive approximation in the Fokker-Planck equation. They claim that the effect of the fluctuating term on outer halo stars in radial orbits is to tear them out of the system, in contradiction with the suggestion by Layzer (1977) that the fluctuating term of the tidal interactions might provide a violent relaxation mechanism for the extended envelopes. Their conclusion is confirmed by both our A and B models, which extend its validity to stronger (closer and slower) encounters.

Tandem encounters are even worse in this sense. As can be clearly seen in the final profiles of models B3 and B9 (Table 3), the first encounter puffs up the system, throwing many stars to the extended halo; being only loosely bound, they are then easily stripped off as a result of the next encounter.

iii) *Inner Regions*

Our simulations show, however, that slow tidal interactions have an interesting effect on layers which are inside the original half-mass-radius. An inner region of $M(R) \propto R$ is built up in the A-cases, while in the B-cases this region is conserved, in absolute units. The corresponding density-profiles and "rotation curves" always become flatter in the inner regions.

The combined effect of both the mass-loss and the "flattening" is to increase the fractional region of $M(R)/R \sim$ const., as is clearly shown in Figure 6. Changes in the mass profile of the A-cases are found to be small for slow hyperbolic encounters ($v_p \gtrsim v_{\text{parabolic}}$), in which the closest approach distance p is larger than $5R_h$, and negligible for distant and faster encounters. They become more and more effective as p decreases; and for $p \sim 3R_h$, say (A3), the resultant flat region of $M(R)/R$ occupies about 65% of the bound mass after a single encounter. Interpenetrating encounters ($p \sim R_h$), especially head-on collisions, seem to be even more effective in producing such a profile, because in such encounters the energy supply to internal degrees of freedom increases rapidly as p decreases, while the mass-loss increases much slower (cf. eqs. [9] and [10] with [11] and [12]). This conclusion holds even when these encounters are fast. However, our one-body-perturber approxi-

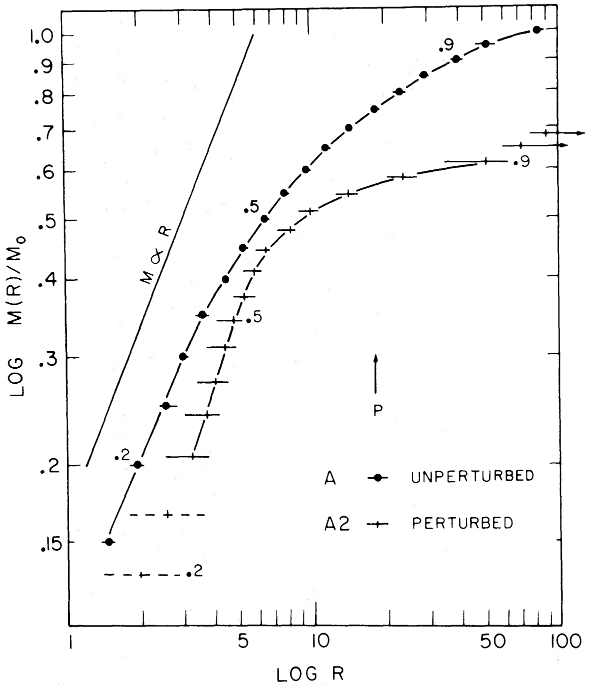

FIG. 5a

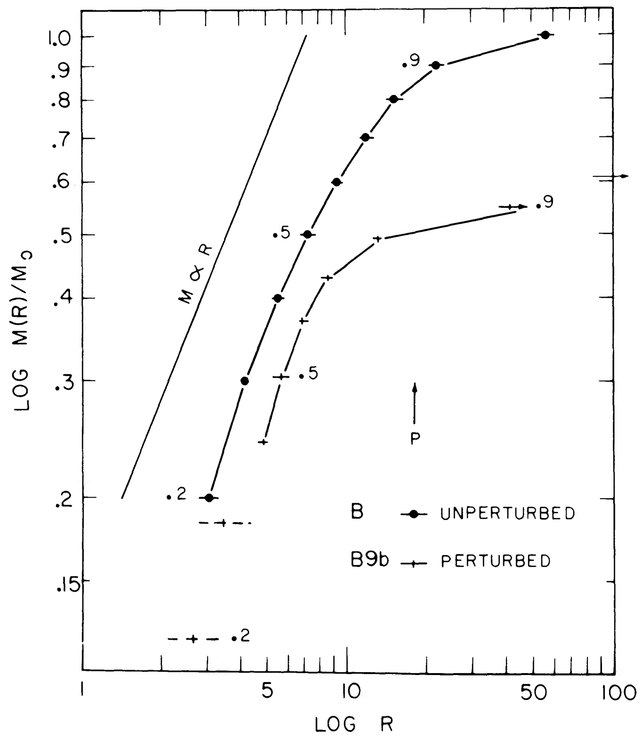

FIG. 5b

FIG. 5.—(a, b) Final mass-profiles of typical models, as evaluated after the encounters and compared with the unperturbed profiles at the same time. The mass, in units of the initial total mass M_0, is shown as a function of the radius, in the absolute units of the experiment. The symbols, which correspond to given fractions of the bound mass, M_b, are the average over three successive crossing-times and the error-bars correspond to temporal deviations. The curves are free-hand interpolations. (a) A-model. $t = 15t_D$. The given fractions of the bound mass are 0.2, 0.25, ..., 1. (b) B-model. A result of tandem encounter. $t = 10t_D$. The given fractions of the bound mass are 0.2, 0.3, ..., 1.

mation probably cannot be representative for such interpenetrating encounters (see § IIIe).

The B-cases, and especially in tandem encounters, show that whenever the system has a significant flat inner region prior to the encounter, it remains flat after it, while the outer parts are stripped, as illustrated in Figures 5b and 6b. As a result of many encounters, the remnant system would become smaller, retaining the flatness of the inner region out to 50–70% of the remnant bound mass.

The important conclusion is that systems which show flat rotation curves over a large fraction of their mass might be produced, and retained as such, by slow hyperbolic tidal encounters in which p is not larger than $5R_h$.

iv) *Expansion or Contraction*

In some cases the resultant system is more extended than the original, and in others it is smaller. We chose to characterize the size of the bound system by its half-mass-radius, R_h, and alternatively by the outer radius which corresponds to 90% of its mass, $R_{0.9}$. The fractional changes in those radii are shown in Figure 7 as functions of the corresponding mass-loss. In general, R_h decreases while $R_{0.9}$ increases, but there are several exceptions.

The tendency to expand is generally stronger in the B cases, as could have been expected from the higher ratio between energy gain and mass loss in those cases (eqs. [9] and [10]). This is probably due to the combined effect of the outer stars being more tightly bound in the B-model, and the second order term of the tidal interaction being dominant there.

The fractional changes in the A-models might be roughly fitted to the straight line

$$\Delta R_h/R_h \approx \Delta M/M \, , \tag{14}$$

but this is not true for most of the B-models. The results for $R_{0.9}$, in which these quantities have opposite sign, are more complicated.

v) *Comparison with Previous Results*

On refitting his numerical results to a King model, Richstone (1975) obtains $\Delta M/M \approx \Delta R_T/R_T$, in which R_T is the tidal radius due to the constant external tidal field from other galaxies in rich clusters. Knobloch (1978a) showed that this result is a direct consequence of the truncation in the energy of the isothermal sphere in the King model, and his argument is valid for the action of both the fluctuating and the secular terms. The systems we investigate are not embedded in a cluster, and there is no external tidal field. Therefore $R_{0.9}$, say, is not directly comparable to the tidal radius of the King model as used by Richstone. His refitting procedure makes it necessary to artifically throw away from the system some stars which are still bound, thus changing the radius of the system. This might explain the discrepancy between our

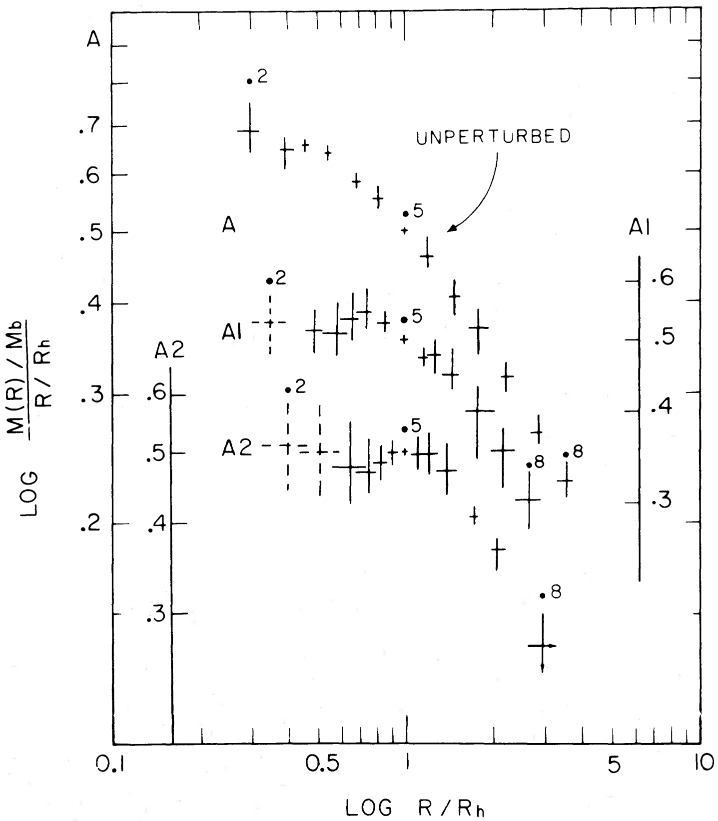

FIG. 6a

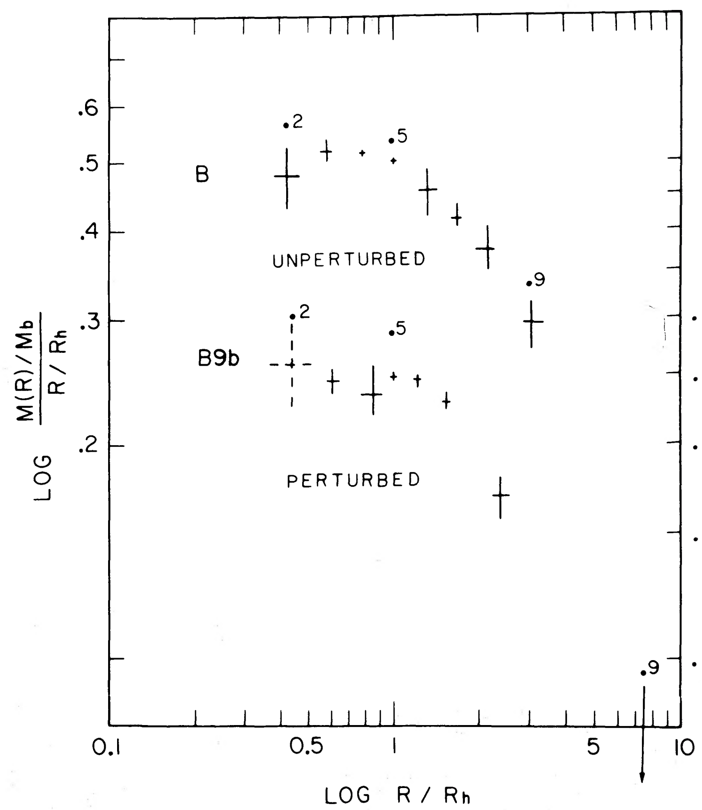

FIG. 6b

FIG. 6.—(*a, b*) "Rotation curves" of final models compared with the unperturbed ones. The mass and the radius are in fractional units relative to the remnant bound system. The error bars have the same meaning as in Fig. 5. The curves are vertically shifted by a factor of $(2)^{1/2}$ relative to each other. (*a*) A-models. The fractional mass-loss is 0.22 in A1 and 0.33 in A2; and the half-mass-radius, R_h, is 5.2 and 4.8 while the unperturbed one is 6.5. Both the fractional and absolute flat regions become more extended in both cases. (*b*) B-model. The fractional mass loss is 0.38 and $R_h \approx 5.63$. The fractional flat region in the "rotation curves" increases, but the absolute region is not changed.

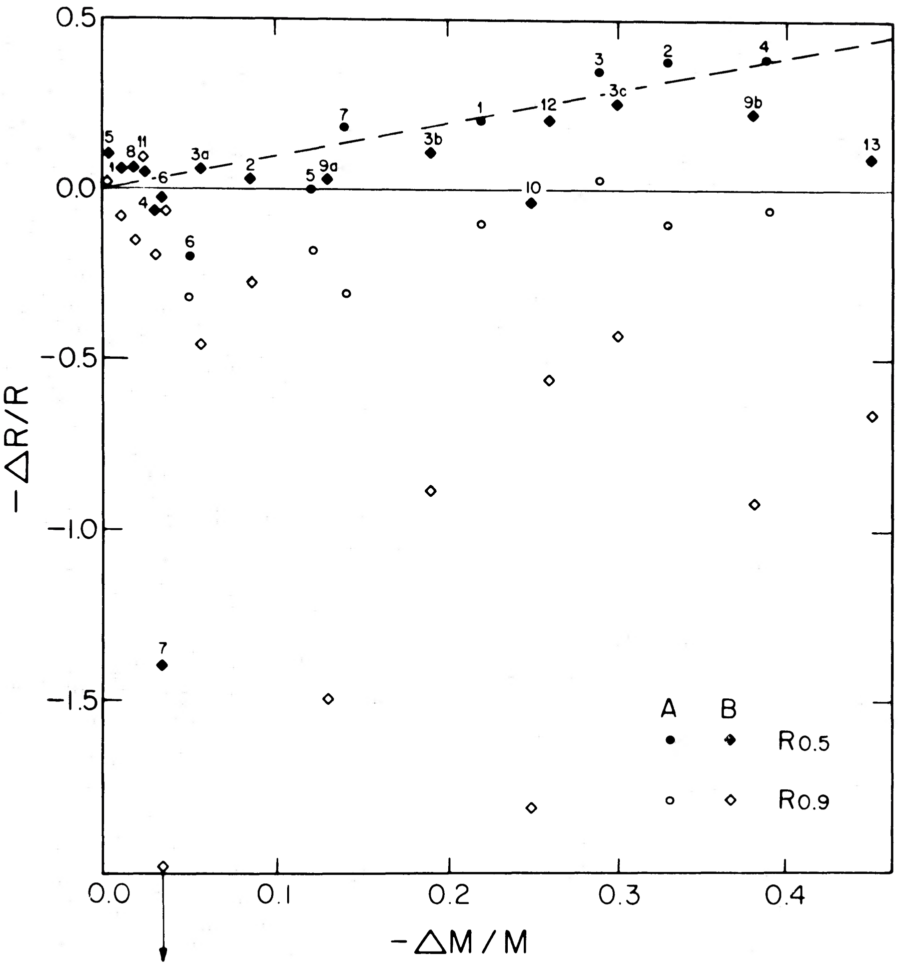

FIG. 7.—Expansion and contraction. The fractional changes in radii corresponding to 50% and to 90% of the bound mass are plotted as functions of the fractional mass-loss, $\Delta M/M$, for models A and B.

results for $R_{0.9}$ and his for R_T. However, there is still an energy gap in our A-model, since the outer stars start off at rest, with some finite negative energy. This might explain (14), according to the lines of argument used by Knobloch (1978*a*). Such an energy gap is much smaller in the B-model, in which the outer stars have some kinetic energy, hence a total energy which is closer to zero, and therefore (14) is not valid for the B-model.

A clue to the flattening that we find in the inner regions might be found in the results of Gutowski and Larson (1976), based on numerical simulations under the restricted three-body approximation. They find for each spherical shell that very roughly $\Delta M/M \propto R^2$ while $\Delta R/R \propto R$, as obtained by averaging the final radii. From their results one can deduce that in the relevant region around R_h, $\Delta(M/R)/(M/R) \approx 4(R/R_h)^2$, which is consistent with the flattening we find.

e) On the Point-Mass Perturber

Perhaps the most important limitation on our results is the representation of the perturber as either a point mass or a system with a small number of bodies, a procedure we took in order to save computer time and memory. With the perturber having so many fewer internal degrees of freedom than it would realistically have, our results for the energy change and the mass loss of the perturbed system may be too crude. For example, on varying the number of bodies in the perturber from one to five the energy gain and mass loss slightly increased in our simulations.

The problem becomes very serious for an interpenetrating encounter, in which $p \leq R_h$. We have carried out a small number of such interpenetrating collisions in order to have some idea about the important effects there. We compared the results with other estimates, but we do not consider the comparisons to be completely representative. In general, we do not expect our results for the energy changes and the mass losses to be substantially affected by this effect as long as $p \geq 2R_h$. This may be qualitatively seen on comparing our results with those obtained by simulating two small N-body systems (Lauberts 1974; Roos and Norman 1979). The qualitative dependence on the encounter parameters is similar, and the magnitudes of the changes are similar to within a factor smaller than

2. Furthermore, as long as we are only interested in qualitative changes in the mass profile, knowledge of exact rates of energy changes and mass losses seems to be unnecessary.

One might still wonder whether a substantial fraction of the material that was disrupted from one system might not become bound to the other system and affect its mass profile. Our simulations show clearly that most of the stripped stars do not become bound to the perturber but rather escape from the two-body system altogether. This effect is stronger for the A-encounters where stellar orbits are elongated, and from which we have deduced our main conclusions regarding the changes in the mass profile. This supports the assumption that our results for the mass profile are qualitatively representative.

IV. DISCUSSION

a) *Rate of Encounters*

Did slow hyperbolic tidal encounters occur frequently enough in the universe to be responsible for the $M \propto R$ profiles? Our simulations show that such encounters affect the mass profile, to produce a flat M/R system, if $p \leq 5R_h$ (hereafter "effective" tidal encounters). A necessary condition for mergers to occur is that the slowly colliding systems ($v_p < 1.16 v_{\text{parabolic}}$) overlap substantially, such that $p \leq 2.5R_h$ whenever the encounter is hyperbolic (cf. White 1978; Fall 1979*a* and references therein). Hence, the geometrical cross section for "effective" tidal encounters, which do not lead to mergers, is much larger than the cross section for penetrating encounters which satisfy the criterion for merger. This simple-minded argument suggests that in any system, in which the subsystems have relative velocities comparable to their internal velocities, the number of "effective" tidal encounters is larger than the number of mergers, provided that the average subsystem spacing is $\gtrsim 5R_h$.

The merger rate in a hierarchical gravitational clustering process, as occurring either with galactic halos or with smaller objects which may cluster to form halos, has been estimated in several ways: White and Rees (1978) have shown analytically that the time scale for a merger of such systems is less than one crossing time of a small (2–8 members) group (see also Fall 1979*b*). Aarseth and Fall (1980), on performing N-body simulations of galaxy merging in a cosmological context and adopting a modest size for galaxies ($R_h \approx 20$ kpc), found that about one-third of the galaxies now in clusters have undergone mergers, mostly in the first generation of their clustering. On assuming a more realistic radius of ~ 50 kpc, one may conclude that practically all of the galactic halos have undergone "effective" tidal encounters in the first stages of their hierarchical clustering, namely, in *small groups*.

Binary galaxies in Turner's sample (1976*a*) have been analyzed by White and Sharp (1977), using White's criterion for merger (1978). They suggested that if Turner's binaries overlap substantially somewhere in their orbits, then they will merge during their next orbital period. In this case they estimated that more than 40% of the galaxies, or even all of them, should have merged in the past—that is, most of them should have recently undergone "effective" encounters. If most of Turner's binaries never overlap substantially, so that their mean true separation $\bar{p}$ is larger than 3 times the mean half-mass radius of the galactic halos, $\bar{R}_h$, one can obtain an upper limit of 58 kpc $h_{50}{}^{-1}$ for $\bar{R}_h$ from the observed $\bar{p} = 173$ kpc $h_{50}{}^{-1}$.

One can try to put a lower limit on the rate of "effective" encounters by a straightforward $n\sigma v$ estimation for "*field*" galaxies. Assume that the geometrical cross section, $\sigma(R_h)$, and the mean velocity dispersion of galaxies, $\bar{v}$, did not change much since the epoch of halo formation $t_{\text{form}}(z_{\text{form}})$. The mean number density at a given cosmological time t, $n(t)$, is a function of the cosmological density parameter Ω_0 and of the mean halo mass. The halo mass is determined by $\bar{R}_h$ via the mean observed rotation velocity, which is assumed to be 250 km s^{-1} (cf. Krumm and Salpeter 1977; Rubin 1980; Dekel and Shaham 1979). The mean free time between "effective" encounters, $\tau(t)$, is estimated to be $[n(t)\sigma\bar{v}]^{-1}$, and we get for the mean number of such encounters for each halo

$$N_{\text{“field”}} \approx \int_{t_{\text{form}}}^{t_0} \frac{dt}{\tau(t)} \approx 0.025\Omega_0(1+z_{\text{form}})^2 \times \left(\frac{\bar{R}_h}{60 \text{ kpc } h_{50}{}^{-1}}\right)\left(\frac{\bar{v}}{300 \text{ km s}^{-1}}\right), \quad (14)$$

on assuming an open universe in the free expansion period.

Unfortunately, uncertainties in (14) are large, so that a definite estimate of $N_{\text{“field”}}$ is impossible at present. The values quoted for $\bar{v}$, for example, range from 50 to 500 km s^{-1}. For $\bar{R}_h$ there is a lower limit coming from the extension of flat rotation curves, and there may be a rough upper limit as was discussed above. A value of 60 kpc $h_{50}{}^{-1}$ seems to be reasonable for the present halos, but they could have been larger in the past, before being stripped by tidal encounters. On assuming that $\Omega_0 \sim 0.1$ and z_{form} is of order 10, one might obtain a number between 0.05 and 1 for $N_{\text{“field”}}$. Formula (14), in fact, underestimates $N_{\text{“field”}}$ because of the focusing effect that was ignored in the simple calculation, where straight lines were assumed for the trajectories. This effect itself might increase σ by a factor of 5. An additional contribution to $n(t)$ might arise from massive dark halos which exist with no visible galaxies in their cores, as were suggested by Rees (1978). Thus, $N_{\text{“field”}}$ does seem to be a number of order unity; in other words, the proposed mechanism might be quite relevant even for "field" halos.

b) *The Merger Picture*

The results of White (1978, 1979) have shown that mergers do not build up an $M \propto R$ profile, but, in fact, destroy it. This seemed to pose a problem for the picture suggested by White and Rees (1978), in which smaller stellar systems (starting with "globular clusters" which were originated by isothermal perturbations) merge to form galactic halos. However, from the larger cross section found here for "effective" tidal encounters, each merger in such a process is followed by several tidal encounters which can reproduce inner $M \propto R$ regions.

Based on the results presented here, we feel that the case is not yet closed even for the mergers themselves. White's results were obtained for fast mergers, which were completed in one single crossing-time. Their resultant profiles, which were almost independent of the initial conditions, may indicate that some kind of violent relaxation took place. We are currently investigating the other extreme case, of adiabatic mergers, where the colliding bodies spiral slowly into each other over many crossing times and undergo a series of semiequilibrium states. Our model A7, which simulates a perturber in a "circular" orbit, indicates that the early stages of such an adiabatic merger indeed assist in flattening the M/R profile, but here a full merger process of identical systems should be simulated. An indication for such a possibility may already be present in the merger simulations of Villumsen (1980).

c) *Tidal Encounters versus Secondary Infall*

The proposed mechanism predicts a correlation between the degree of clustering of a galaxy (be it a field galaxy, a member of a small group, or a member of a large one) and the *fractional* extension of its $M \propto R$ region. This correlation could not be extended to rich clusters, where galaxies should have lost most of their halos, as discussed below. Secondary cosmological infall (Gunn 1977; Gott 1977) should lead to a similar correlation.

A simple test might be suggested in order to distinguish between cosmological infall and slow tidal interactions between galactic halos, as mechanisms responsible for the $M \propto R$ profiles in relatively isolated halos. In the former case the more massive halos, which have accreted more cosmological material, should possess more extended regions of $M \propto R$. In the tidal picture, the inverse may be true. On assuming that halos were originally formed in similar sizes and masses, the less massive ones at present should have undergone more tidal encounters, and hence should contain a larger fractional region of $M \propto R$. The mass, in this connection, might be determined by the magnitude of the constant rotation velocity. If tidal interactions are occurring, then one might observe such structural differences also between close and distant halos. We should, however, point out that if the tidal mechanism is acting during the formation of the halo out of smaller objects, we would not be able to observe such structural changes and all the halos should have similar shapes.

In any case in which collisions take place within a larger, bound, density perturbation (such as a galactic halo in formation from smaller objects; a group or a cluster of galaxies), the material that becomes unbound might form a common envelope (a diffuse background halo?). That material can later supply dissipationless material for secondary infall, which will produce even more extended envelopes around the subsystems. Here, the two proposed mechanisms may act together to produce the observed flat rotation curves (Dekel, Kowitt, and Shaham 1980).

d) *Halos in Rich Clusters*

If clusters of galaxies were formed by hierarchical gravitational clustering, the halos were interacting via slow encounters at the early stages of their clustering, where tidal effects tended to flatten their density profiles along the lines suggested above. However, our simulations show that stripping is large in each encounter and, in fact, indicate that it becomes a *runaway* effect in case of many encounters. This is seen from the fact that, as a result of such encounter, each "shell" of stars finds itself at a larger radius (cf. Fig. 5), so that most parts of the system, excluding, perhaps, a central (10%) core, become less bound, an easy target for further stripping. It is expected, therefore, that galaxies now in clusters have lost most of their halos due to successive encounters during their clustering process.

Note that there is substantial stripping due to fast collisions as well (cf. Gallagher and Ostriker 1972; Richstone 1975; and other references mentioned above) so that one does not expect to find very extended halos attached to cluster galaxies also in case that clusters were formed by collapse of adiabatic perturbations (Doroshkevich, Sunyaev, and Zel'dovich 1974) or by a combined process of collapse and clustering (adiabatic and isothermal perturbations; cf. Dekel and Shaham 1980*a*).

e) *Further Applications*

In some respects, the problem studied here is similar to the problem of tidal shocks in globular clusters moving through the disk of the galaxy. (This was pointed out to us by M. J. Rees and J. P. Ostriker.) Although it is still uncertain whether these cause the centers of the clusters to contract or to expand, the runaway effect suggested above should cause complete disruption of most other parts of the clusters, as was previously suggested by Spitzer and Chevalier (1973).

Our results for slow encounters might also be relevant to various other scenarios for galaxy formation. Fall (1979*b*), for example, sketched a picture of elliptical galaxies forming by mergers of spirals. His assumptions, that the halos merge to a common halo prior to the merger of the visible cores, are consistent with our results for the high rate of mass loss in the outer envelopes. Larson, Tinsley, and Caldwell (1980) suggested that the gas in spirals, which was exhausted by star formation, has been replenished by infall from residual envelopes, and that S0's may be disk systems that lost their gas-rich envelopes at an early stage when the clusters collapsed. The required gaseous envelopes might be contracting quasi-statically within a massive dark halo (cf. Rees and Ostriker 1977; Rees 1978). Tidal encounters, slow or fast, may cut the gas supply by stripping the galaxies from their halos, and lead to S0's. A basic difference between spirals and S0's might, therefore, be the presence or lack of massive halos around them.

Based on the (surprisingly) weak correlation between B–V and M/L_B in spiral galaxies, Tinsley (1980) suggested the possibility that the dark mass is relatively more dominant in later Hubble type galaxies ("blue" disks with small nuclear bulges) than in early type galaxies ("red" disks with significant bulges). If dark halos form first and gas then condenses in their potential wells (White and Rees, 1978), then the type of the resultant visible galaxy might be, indeed, determined by the relative dominance of the dark halo. It is possible, that gas fragments into stars only when its self-gravity overcomes the external halo potential (Larson, 1976; Fall and Efstathiou, 1980; Tinsley, 1980). A centrally condensed halo might thus inhibit star formation and the gas will settle to a disk, while a loosely bound halo would allow efficient star formation during the collapse, leading to a significant bulge.

The tidal encounters studied here might provide a mechanism for the expected structural differences between halos. They first form as centrally condensed objects. Slow tidal encounters make then most of their parts less bound. At 20% of the mass, say, the mean density may drop by a factor of 5 due to one encounter (see Figure 5*a*). Thus, late type spirals should mostly form in field halos, while earlier types should form inside more clustered halos, which were subject to more encounters. One may even extend this idea to understand this formation of S0s and Ellipticals in rich clusters, where halos should be very loosely bound due to many encounters (Dekel and Hoffman 1980).

We especially thank Sverre J. Aarseth for kindly making his N-body code available to us. We also thank M. S. Fall, D. Lynden-Bell, J. P. Ostriker, and M. J. Rees for helpful comments.

REFERENCES

Aarseth, S. J. 1972, in *Gravitational N-Body Problem*, ed. M. Lecar (Dordrecht: Reidel), p. 373.
Aarseth, S. J., and Fall, S. M. 1980, *Ap. J.*, **236**, 43.
Aarseth, S. J., and Lecar, M. 1975, *Ann. Rev. Astr. Ap.*, **13**, 1.
Ahmad, A., and Cohen, L. 1973, *J. Comp. Phys.*, **12**, 389.
Alladin, S. M. 1965, *Ap. J.*, **141**, 768.
Bergeron, J., and Gunn, J. E., 1977, *Ap. J.*, **217**, 892.
Bouvier, P. 1971, *Astr. Ap.*, **14**, 341.
Bouvier, P., and Janin, G. 1970, *Astr. Ap.*, **9**, 461.
Contopoulos, G., and Bozis, G. 1964, *Ap. J.*, **139**, 1239.
Da Costa, L. N., and Knobloch, E. 1979 *Ap. J.*, **230**, 639.
Dekel, A., and Hoffman, Y. 1980, preprint.
Dekel, A., Kowitt, M., and Shaham, J. 1980, in preparation.
Dekel, A., and Shaham, J. 1979, *Astr. Ap.*, **74**, 186.
———. 1980*a*, *Astr. Ap.*, in press.
———. 1980*b*, preprint.
Doroshkevich, A. G., Sunyaev, R. A., and Zel'dovich, Ya. B. 1974, in *IAU Symposium 63, Confrontation of Cosmological Theories with Observational Data*, ed. M. S. Longair (Dordrecht: Reidel), p. 213.
Faber, S. M., and Gallagher, J. S. 1979, *Ann. Rev. Astr., Ap.*, **17**, 135.
Fall, S. M. 1978, *M.N.R.A.S.*, **185**, 165.
———. 1979*a*, *Ann. NY Acad. Sci.*, in press.
———. 1979*b*, *Nature*, **281**, 200.
Fall, S. M., and Efstathiou, G. 1980, preprint.
Gallagher, J. S., and Ostriker, J. P. 1972, *A.J.*, **77**, 288.
Gott, J. R. 1973, *Ap. J.*, **186**, 481.
———. 1975, *Ap. J.*, **201**, 296.
———. 1977, *Ann. Rev. Astr. Ap.*, **15**, 235.
Gott, J. R., and Turner, E. L. 1976, *Ap. J.*, **209**, 1.
Gunn, J. E. 1977, *Ap. J.*, **218**, 592.
Gutkowski, W. J., and Larson, R. B. 1976, *Pub. A.S.P.*, **88**, 374.
Hénon, M. 1964, *Ann. d'Ap.*, **27**, 83.
Kirshner, R. D. 1977, *Ap. J.*, **212**, 319.
Knobloch, E. 1978*a*, *Ap. J.*, **222**, 779.
———. 1978*b*, *Ap. J. Suppl.*, **38**, 253.
Krumm, N., and Salpeter, E. E. 1977, *Astr. Ap.*, **56**, 465.
Larson, R. B. 1974*a*, *M.N.R.A.S.*, **166**, 585.
———. 1974*b*, *M.N.R.A.S.*, **169**, 229.
———. 1975, *M.N.R.A.S.*, **173**, 671.
———. 1976, *M.N.R.A.S.*, **176**, 31.
Larson, R. B., Tinsley, B. M., and Caldwell, C. N. 1980, *Ap. J.*, **237**, 692.
Lauberts, A. 1974, *Astr. Ap.*, **33**, 231.
Layzer, D. 1977, *Gen. Rel. Grav.*, **8**, 3.
Ostriker, J. P., and Peebles, P. J. E. 1973, *Ap. J.*, **186**, 467.
Ostriker, J. P., Peebles, P. J. E., and Yahil, A. 1974, *Ap. J.* (*Letters*), **193**, L1.
Peebles, P. J. E. 1970, *A.J.*, **75**, 13.
———. 1980, *Physical Cosmology* (New York: Gordon & Breach), in press.
Rees, M. J. 1978*a*, *Phys. Scripta*, **17**, 371.
———. 1978*b*, in *The Evolution of Galaxies and Stellar Populations*, ed. B. M. Tinsley and R. B. Larson (New Haven: Yale University Observatory), p. 339.
Rees, M. J., and Ostriker, J. P. 1977, *M.N.R.A.S.*, **179**, 541.
Richstone, D. O. 1975, *Ap. J.*, **200**, 535.
Roberts, M. 1975*a*, in *Stars and Stellar Systems*, Vol. **9**, ed. A. and M. Sandage and J. Kristian (Chicago: University of Chicago Press), p. 309.
———. 1975*b*, in *IAU Symposium 69*, *Dynamics of Stellar Systems*, ed. A. Hayli (Dordrecht: Reidel).
Roos, N., and Norman, C. A. 1979, *Astr. Ap.*, **76**, 75.
Rubin, V. C. 1978, *Comments Ap.*, **8**, 79.
———. 1980, preprint.
Rubin, V. C., Ford, W. K., and Thonnard, N. 1980, preprint.
Sastry, G., and Alladin, S. M. 1970, *Ap. Space Sci.*, **7**, 261.
———. 1977, *Ap. Space Sci.*, **46**, 285.
Spitzer, L. 1958, *Ap. J.*, **127**, 17.
Spitzer, L., and Chevalier, R. A. 1973, *Ap. J.*, **183**, 565.
Tinsley, B. M. 1980, preprint.
Turner, E. L. 1976*a*, *Ap. J.*, **208**, 20.
———. 1976*b*, *Ap. J.*, **208**, 304.
van Albada, T. S., and van Gorkom, J. H. 1977, *Astr. Ap.*, **54**, 121.
Villumsen, J. V. 1980, preprint.
White, S. D. M. 1978, *M.N.R.A.S.*, **184**, 185.
———. 1979, *M.N.R.A.S.*, in press.
White, S. D. M., and Rees, M. J., 1978, *M.N.R.A.S.*, **183**, 341.
White, S. D. M., and Sharp, N. A. 1977, *Nature*, **269**, 395.
Yahil, A. 1977, *Ap. J.*, **217**, 27.

AVISHAI DEKEL and JACOB SHAHAM: Racah Institute of Physics, Hebrew University of Jerusalem, Jerusalem, Israel

MYRON LECAR: Center for Astrophysics, Smithsonian Institution, 60 Garden Street, Cambridge, MA 02138